Petrographic and Geochemical Characterization of the Metasedimentary rocks in the southern part of Ouaddaï (eastern Chad): Source, Provenance and Tectonic Setting.

Félix Nenadji Djerossem[1], Moussa Isseini[2], Malik Hisseine Malik[3], Issaka Ousman Al-Gadam[2]

Abstract

The southern part of Ouaddaï (eastern Chad), is part of the Central African Orogenic Belt (CAOB), composed mainly of metasedimentary rocks affected by low (green schist) to medium (amphibolite) grade metamorphism. Petrographic and geochemical data are used to understand their origin and tectonic environment. Paragneisses, metapelites and phengite quartzites are mostly derived from greywackes and arkoses. CIA and $A1_2O_3$-CaO + Na_2O-K_2O values indicate a low to intermediate degree of weathering. Th/U, PIA and CIW values suggest a low to intense weathering degree. LREE enrichment, the negative Eu anomaly and the La/Sc ratio show that these metasedimentary rocks are originated from a felsic source rock. The geochemical characteristics of these metasedimentary rocks are similar to those of Archean to post-Archean upper continental crust. The original sedimentary rocks were probably deposited in an active to passive continental margin tectonic environment.

Keywords: Metasedimentary rocks, Ouaddaï massif, Central African Orogenic Belt, post-Archean upper continental crust.

Résumé

La partie sud du Ouaddaï (Tchad oriental), située au nord du Craton du Congo, fait partie de la Ceinture Orogénique d'Afrique Centrale (COAC), constituée majoritairement de roches métasédimentaires, affectées par un métamorphisme de faible (schiste vert) à moyen (amphibolite) degré. Les données pétrographiques et géochimiques sont utilisées pour comprendre leur provenance et leur environnement tectonique. Les paragneiss, les métapelites et les quartzites à phengite dérivent dans la plupart des cas des grauwackes et des arkoses. Les valeurs de CIA et $A1_2O_3$-CaO + Na_2O-K_2O indiquent un degré d'altération faible à intermédiaire. Celles de Th/U, PIA et CIW, suggèrent un degré d'altération faible à intense. L'enrichissement en LREE, l'anomalie négative en Eu et le rapport La/Sc montrent que ces roches métasédimentaires proviennent d'une roche mère de composition felsique. Les caractéristiques géochimiques de ces roches métasédimentaires se rapprochent de celles de la croûte continentale supérieure, archéenne à post-archéenne. Les roches sédimentaires d'origine se sont probablement mises en place dans un environnement tectonique de type marge continentale active à passive.

Mots clés : Roches métasédimentaires, Massif du Ouaddaï, Ceinture Orogénique d'Afrique Centrale, croûte continentale post-archéenne.

[1]Department of Mining, New and Renewable Energies, National Higher Institute of the Sahara and Sahel, Iriba, Chad.
[2]Department of Geology, Faculty of exact and applied Sciences of Farcha, University of N'Djamena,, B.P. 1027, N'Djamena, Tchad. E-mail:
[3]Laboratory of Geosciences, Natural Resources and Environment, University of Douala, BP: 44155, Douala, Cameroon.

*Corresponding: Djerossem@gmail.com

1. Introduction

Chad is located to the north of the Congo Craton (Figure 1A) and forms part of the Central African Orogenic Belt (COAB), made up of a collection of rocks formed during the Pan-African orogeny towards the end of the Precambrian (700-520 Ma; Bessoles and Trompette, (1980)). The Precambrian basement formations exposed in Chad are divided into five small massifs (Figure 1B): the Tibesti massif in the north, the Ouaddaï massif in the east, the Guéra massif in the south-central region, the Mayo Kebbi massif in the south-west and the Baïbokoum massif in the south. Several petrographic and geochemical studies have been carried out on the granitoids to understand the geodynamic evolution of the crust exposed in these massifs. Unfortunately, very little attention has been given to metasedimentary rocks, which can also be used to determine the weathering intensity, the tectonic environment and the composition of the source zone of metasedimentary rocks (Armstrong-Altrin et al., 2004a, b, 2015a, b; Verma et al., 2016; Ngoniri et al., 2020; Amelle et al., 2023; Miryam et al., 2023; Bhatia and Crook 1986; McLennan et al.,1993; Cullers, 2000; Zeng et al., 2019). Petrographic and geochemical studies of major, trace and rare earth elements are highly effective approaches for assessing the Weathering intensity, provenance and tectonic environment of metasedimentary rocks. (McLennan et al. (1993, 1995).

In this paper, we present first petrographic and geochemical data to determine the geodynamic environment and provenance of the metasedimentary rocks of the southern Ouaddaï.

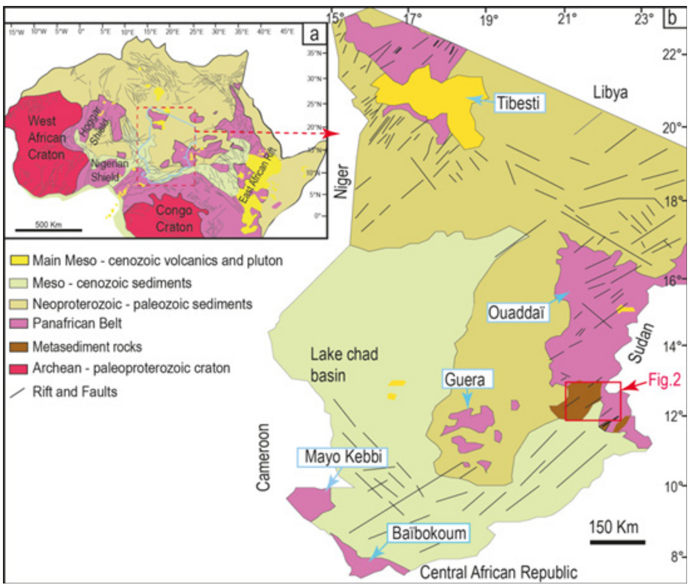

Figure 1: a) Tectonic Map of Africa, and location of Chad in the African geological context. The main geologic features of Africa are indicated (modified after Kogbe, 1981, and Milesi et al., 2010).

b) Geological map of Chad showing the main Pan-African massifs.

2. Geological setting

The Ouaddaï massif (eastern Chad) is part of the Central African Orogenic Belt (CAOB), which stretches from Cameroon through Central African Republic (CAR) and Chad (Djerossem et al., 2020). The basement of the Ouaddaï massif is dominated in its northern half by a wide variety of granites (biotite anatexis granite, biotite and amphibole granite, two-mica anatexis granite) and migmatites, associated with very rare granodiorites and diorites. The metamorphic formations are represented by amphibolites, gneisses, schists and quartzites in the form of enclaves. The southern half of Ouaddaï (Figure 2) is dominated by: (a) an Archean to Mesoproterozoic meta-sedimentary series, recrystallized under green schist facies and amphibolite conditions (Djerossem et al., 2020, 2021).

This series is characterized by a composite NE-SW-trending S_0/S_{1-2} foliation associated with centimeter to hectometer scale P_1 and P_2 isoclinal folds and bearing a weak NW dipping L_{1-2} lineation. This foliation is also affected by straight open folds P_3 associated with axial plane schistosity S_3 dipping steeply to the NNW or NW. This series, derived from erosion of the surrounding cratons, is intercalated by : (a) mafic magmas in the form of amphibolite; (b) a high-K to shoshonitic calc-alkaline series that intrudes the metasedimentary series, consisting of peraluminous leucogranite batholiths (635 ±3Ma) and plutons of pyroxene monzonite, hornblend granodiorite, biotite granite (540 ±5Ma) and muscovite-garnet leucogranite (613 ±8Ma). According to Djerossem et al. (2020, 2021), the southern part of the Ouaddaï was formed a continental back-arc basin, characterized by a high geothermal gradient inducing partial melting of the middle to lower crust around 635-612 Ma. After the tectonic inversion (resumption in compression of a passive margin, characterized by intense deformation of the margin and the oceanic basin, generating structures such as folds, faults, deposition of terrigeneous sediments and plutons), the final phase of the Pan-African orogeny was marked, south of the Ouaddaï and on the scale of the CAOB, by the emplacement of the highly potassic to shoshonitic pluton typical of the post-collisional series.

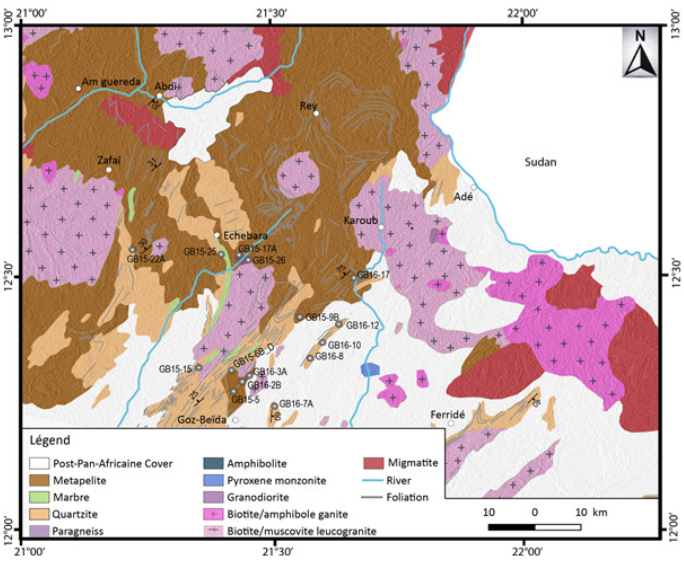

Figure 2: Geological map of the study area (Gsell et Sonnet, 1960; modified after Djerossem et al., 2020) and sampling sites.

3. Analytical methods

Selected metasediment rocks samples were sawn (at the Geosciences and Environment Laboratory in Toulouse, GET) to prepare thin sections and cut into small blocks for geochemical investigations. Approximately 200 to 500 g of each sample was ground in a steel jaw crusher and then pulverised with an agate ball mill. The powders were digested using an alkaline fusion procedure where the powder was mixed with lithium metaborate and melted to produce a glass pellet. The pellet was digested in dilute nitric acid prior to analysis. Analyses and digestions were carried out at the ''Service d'Analyse des Roches et Minéraux (SARM, CRPG, France)''; major elements were determined by ICP-OES while trace elements were determined by ICP-MS following the procedure described in Carignan et al. (2001).

4. Petrography

4.1. Paragneiss

They fall into three categories according to their mineralogical composition:

Garnet-biotite paragneiss outcrops in slabs, characterized by dark to greyish levels that highlight schistosity (Figure 3a). It has a granolepidoblastic texture (Figure 3b), composed of quartz + garnet + biotite ± plagioclase + opaque minerals. Quartz (30-40%) forms the matrix of the rock. Garnet (15-25%) is automorphic to subautomorphic and shows large patches marked by numerous fractures filled by biotite. Biotite (10-15%) occurs as inclusions in garnet and sometimes between quartz grains. Plagioclase (5-10%) is automorphic to subautomorphic and has a more or less altered surface.

Amphibole paragneiss occurs in centimetric to metric slabs and is consistent with the foliation of the métapelites (Figure 3c). At the fracture, it is characterized by light levels of quartz and plagioclase and dark levels rich in ferromagnesian minerals. It has a nematoblastic to granolepidoblastic texture (Figure 3d), composed of amphibole + phengite + quartz + feldspar + plagioclase + epidote + sphene. Amphibole (20-40%) is an actinote and occurs as a more or less elongated rod. Some very fine amphibole crystals are embedded in a quartz-feldspar matrix. Phengite (10-20%) occurs as microcrystals moulding the feldspar porphyroclasts. Feldspar (10-15%) occurs in the form of more or less altered boudins containing inclusions of phengite, quartz and opaque minerals. Quartz (5-10%) is xenomorphic and forms the matrix with plagioclase (5-8%). Sphene (< 2%) is automorphic and lozenge-shaped, moderately cracked. It is associated with actinote crystals. Epidote (< 2%) occurs as elongated crystals and may be derived from the transformation of amphibole.

Calcium silicate paragneiss outcrops in slabs near a watercourse and characterized by a brownish to dark alteration (Figure 3e and f). It has a granoblastic texture (Figure 3g and h), composed mainly of amphibole + pyroxene + quartz + garnet + feldspar + plagioclase + calcite. Secondary minerals include epidote, sphene, prehnite and zircon. Amphibole (20-30%) shows a preferential orientation highlighting foliation. Some crystals are partially retromorphosed into chlorite. Pyroxene (15-25%) is a diopside and occurs as subautomorphic to automorphic phenocrysts. Quartz (10-20%) is oriented parallel to the foliation. Garnet (8-10%) occurs in more or less fractured phenocrysts and contains plagioclase and quartz inclusions. Feldspar (< 8%) occurs in more or less altered phenocrysts. Plagioclase (< 6%) is an albite and occurs as slightly altered phenocrysts. Calcite (< 5%) has elongated sections characterized by lamellar polysynthetic macles. Epidote (< 2%) is multi-coloured and locally associated with calcite and clinopyroxenes. Sphene (1%) is rhombic and occurs as inclusions in amphibole crystals.

4.2. Metapelite

These outcrop in small hills or slabs and are light grey or black in color, composed of micas and quartz (Figure 3i). They are intersected by lenticular and curled quartz veins transposed in the foliation and microfractures. These structures indicate a succession between brittle and ductile deformation. Microscopically, the metapelites have a grano-lepidoblastic texture (Figure 3j, k and l), with light beds of quartz alternating with dark beds rich in micas (phengite and biotite). Garnet and tourmaline are also present in some thin sections. Secondary minerals include monazite, zircon and opaque minerals. Quartz (30-45%) forms the matrix of the rock and is characterized by the presence of grains with lobed edges indicating recrystallization at high temperature. Phengite (20-35%) is oriented parallel to the foliation and contains monazite inclusions and opaque minerals. Garnet crystals (10-15%) are moulded by phengite and biotite. They are fractured and contain inclusions of biotite and quartz. Biotite (5-10%) is interstitial between quartz minerals and phengite. It highlights a schistosity plane parallel to the foliation plane. Tourmaline (< 3%) is a prismatic automorph with transverse fractures. Monazite (1%) is included in micas, while epidote (1%) is associated with phengite crystals.

4.3. Phengite quartzite

They are mostly associated with metapelites and outcrop in slabs, blocks or small hills, brownish to white in color and in some places forming NE-SW trending ridges (Figure 3m). They are cross-cutted by veins of boudin quartz that run parallel to the foliation. They have a granolepidoblastic texture (Figure 3n, o and p) and are composed of quartz, phengite, tourmaline, garnet and sillimanite. Secondary minerals include zircon and opaque minerals. Quartz (40-50%) forms large patches and is marked by the presence of lobed grain boundaries indicating dynamic recrystallization at high temperature (Hirth and Tullis, 1990; Dunlap et al., 1995). Phengite (15-25%) emphasises the foliation and locally contains opaque mineral inclusions. Tourmaline (5-15%) is marked by an elongated section with transverse microfractures. Garnet (5-10%) is locally moulded by phengite. Sillimanite (5-10%) appears as an elongated rod following the plane of the foliation.

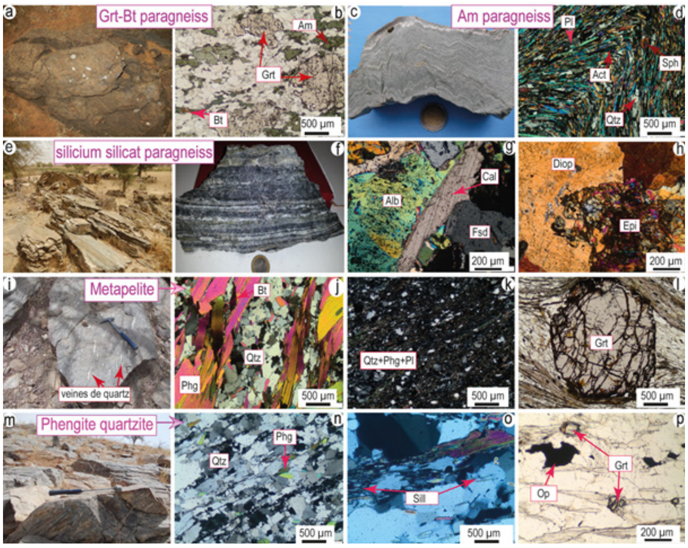

Figure 3: Macro and micro-photographs of metasedimentary rocks from Southern Ouaddaï. (a and b) grenat-biotite paragneiss ; (c and d) amphibole paragneiss ; (e, f, g and h) silicium silicat paragneiss; (i, j, k and l) metapelite and (m, n, o and p) phengite quartzite. Am =Amphibole; Grt = Grenat; Bt = Biotite; Phg = Phengite; Qtz = Quartz; Sill = Sillimanite; Pl = Plagioclase; Fsd = Feldspar; Act = Actinote; Cal = Calcite; Alb = Albite; Diop = Diopside, Epi = Epidote; Sph = Sphene; Op = Opaque.

5. Geochemitry

5.1. Classification of metasedimentary rocks

The geochemical data of representative fresh analyzed samples of the southern part of Ouaddaï metasedimentary rocks are displayed in Table 1. In the discrimination diagram of Winchester et al. (1980), all the samples fall into the sedimentary rock field (Figure 4a). The classification diagram by Herron et al. (1988), shows that the southern Ouaddaï metasedimentary rocks correspond mainly to greywackes and arkoses (Figure 4b).

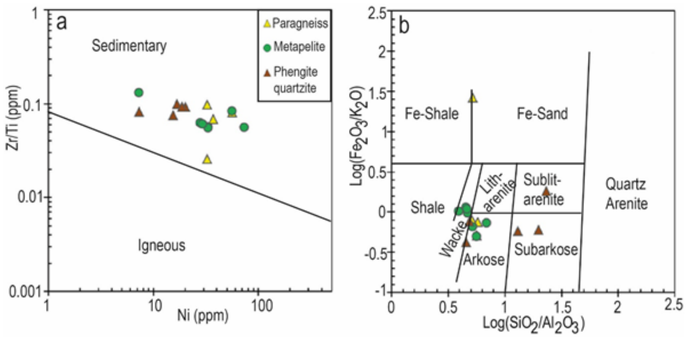

Figure 4: Zr/Ti vs Ni protolith discrimination diagram (after Winchester et al., 1980); b) Sediment classification diagram (after Herron and al., 1988).

5.2. Major elements

Paragneisses are characterized by SiO_2 concentrations ranging between 56.07 to 57.67%. Al_2O_3 concentrations range from 9.69 to 10.91%, with Fe_2O_3 (2.95 - 4.53%), MgO (7.28 - 9.75%) and TiO_2 (0.41 - 0.51%) respectively. The K_2O and CaO contents are 0.17 to 6.71% and 9.13 to 17.32% respectively. P_2O_5 (0.09 - 0.18%) and MnO (0.07 - 0.14%) concentrations are relatively low. The alkaline content (Na_2O + K_2O) range from 2.48 to 7.43% respectively.

Metapelites are characterized by high contents of SiO_2 (64.34

- 77.10%), Al_2O_3 (11.29 - 16.45%) and Fe_2O_3 (2.90 - 6.67%) with low contents of MgO (0.18 - 1.80%), CaO (0 - 0.55%) and Na_2O (0.11 - 0.99%) compared to paragneisses. P_2O_5 and MnO contents are 0 to 0.10% and 0.01 to 0.02% respectively. K_2O concentrations ranging between 4.41 to 6.47% and alkaline concentrations ($Na_2O + K_2O$) range from 4.52 to 8.61%.

Phengite quartzites are characterized by relatively high concentrations of SiO_2 (70.61 - 92.56%) and Al_2O_3 (3.98 - 15.44%). The concentrations of Fe_2O_3 (0.85 - 2.22%), MgO (0.12 - 1.12%) and CaO (0 - 1.89%) are relatively low. Na_2O and K_2O contents ranging from 0.07 to 4.96% and from 1.13 to 3.84% respectively. TiO_2 (0.08 - 0.23%), P_2O_5 (0 - 0.08%) and MnO (0 - 0.04%) contents are very low in the rock. Alkaline concentrations ($Na_2O + K_2O$) range from 1.21 to 8.29%.

5.3. Trace and rare earth elements

Trace element and rare earth elements concentrations of the southern part of Ouaddaï are displayed in Table 1. The paragneisses are characterized by LILEs (Ba, Rb and Sr) contents from 89.98 to 1441ppm; from 8.324 to 131.5ppm and from 89.54 to 194.5ppm respectively. The ferromagnesian elements and incompatible elements concentrations are: Sc (7.48 - 13.70ppm); V (36.68 - 56.03ppm); Cr (65.13 - 113.30ppm); Co (8.06 - 11.09ppm) and Ni (32.42 - 56.37ppm). The REE pattern normalized to chondritic values (Figure 5a) show an enrichment of light REE [$(La/Yb)_N$ = 5.78 - 13.56] compared to heavy REE [$(Gd/Yb)_N$ = 1.42 - 1.67]; These paragneisses show a negative Eu anomaly (Eu/Eu = 0.66 - 0.69; Figure 5a) and are identical to the Upper Continental Crust (UCC) and the Post-Archean Australian Shale (PAAS).

In the metapelites, Ba (489.70 - 2201.17 ppm) and Rb (139.21 - 328.26 ppm) concentrations are slightly higher than those observed in the paragneisses, while Sr (31.92 - 198.02 ppm) contents are identical to the latter. The concentrations of Sc (7.72 - 14.25 ppm); V (14.65 - 226.87ppm); Cr (75.64 - 419.6 ppm); Co (3.80 - 15.43 ppm) and Ni (7.26 - 72.69 ppm) are relatively identical to those of paragneisses. The REE pattern normalized to chondritic values show an enrichment of LREE [$(La/Yb)_N$ = 5.33 - 15.73] compared to HREE [$(Gd/Yb)_N$ = 1.08 - 1.85]. The metapelite samples show a negative Eu anomaly (Eu/Eu = 0.64 - 0.97; (Figure 5b) and are identical to the Upper Continental Crust (UCC) and the Post-Archean Australian Shale (PAAS).

In the phengite quartzites, the Ba, Rb and Sr contents ranging from 177.46 to 955.40 ppm; from 48.97 to 137.30 ppm and from 21.07 to 171.39 ppm respectively. These values are similar to those of the previous rocks. The concentrations of Sc (2.57 - 3.28 ppm); V (14.37 - 37.44 ppm); Cr (63.34 - 234.26 ppm); Co (0.95 - 3.89 ppm) and Ni (7.37 - 20.35 ppm) are slightly lower than those of the paragneisses and metapelites. The REE pattern normalized to chondritic values show an enrichment of LREE light [$(La/Yb)_N$ = 8.88 - 31.03] compared to HREE [$(Gd/Yb)_N$ = 1.30 - 2.88]. These phengite quartzites show a negative Eu anomaly (Eu/Eu = 0.58 - 1.01; Figure 5c) and are identical to the Upper Continental Crust (UCC) and the Post-Archean Australian Shale (PAAS).

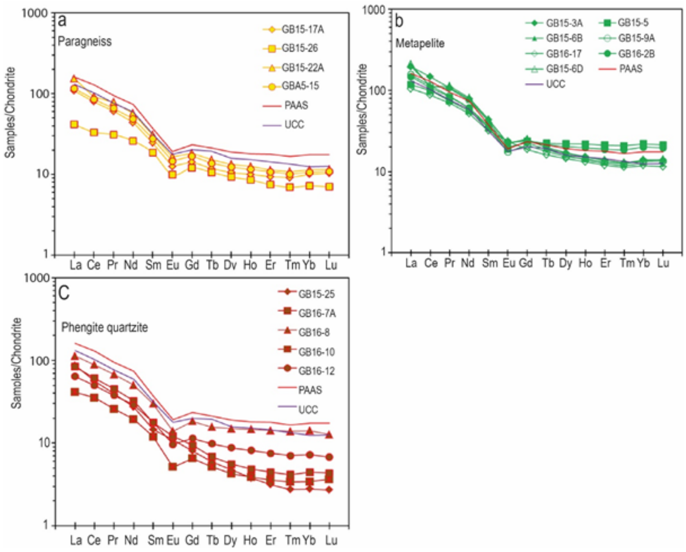

Figure 5: Chondrite-normalized REE metasedimentary rocks of southern Ouaddaï compared to PASS and UCC.

Table 1: Major and trace-element geochemistry of selected samples.

	paragneiss				Metapelite							Phengite quartzite				
	GB15-17A	GB15-26	GB15-22A	GB15-15	GB16-3A	GB15-5	GB15-6B	GB15-9A	GB16-17	GB16-2B	GB15-6D	GB16-7A	GB16-8	GB16-10	GB16-12	GB15-25
wt%																
SiO_2	56.41	56.07	56.25	57.67	64.34	68.53	68.65	68.71	70.35	75.13	77.10	70.61	88.26	90.99	92.56	71.47
Al_2O_3	9.69	10.69	10.91	10.22	16.45	15.25	14.65	14.86	12.65	14.56	11.29	15.44	6.76	4.56	3.98	14.68
Fe_2O_3	2.98	4.49	4.53	3.43	6.67	6.26	5.80	5.99	5.80	2.90	5.27	1.62	1.18	0.85	2.02	2.22
MgO	9.61	7.28	9.75	9.16	1.80	0.80	1.77	1.55	0.46	0.18	1.04	0.43	0.12	0.18	0.15	1.11
CaO	15.37	17.52	9.15	9.88	0.05	0.00	0.00	0.07	0.55	0.00	0.00	1.89	0.00	0.00	0.00	1.19
Na_2O	1.76	2.51	0.79	0.72	0.15	0.14	0.11	0.14	0.99	0.52	0.11	4.45	0.15	0.07	0.09	4.96
K_2O	3.95	0.17	3.75	6.71	6.47	5.43	5.88	5.50	7.62	4.42	4.41	3.84	2.02	1.44	1.13	2.90
TiO_2	0.41	0.51	0.46	0.43	0.64	0.69	0.55	0.57	0.41	0.50	0.55	0.23	0.17	0.08	0.18	0.23
P_2O_5	0.16	0.09	0.11	0.10	0.00	0.00	0.00	0.05	0.10	0.00	0.00	0.00	0.00	0.00	0.00	0.08
MnO	0.07	0.14	0.07	0.06	0.02	0.02	0.01	0.02	0.02	0.02	0.02	0.03	0.00	0.00	0.04	0.04
LOI	0.59	0.41	1.46	0.93	2.26	2.50	2.64	2.24	0.95	2.35	1.71	0.58	1.10	0.94	0.77	1.22
SUM	99.00	99.47	99.19	99.53	98.86	99.80	100.04	99.47	97.89	100.37	99.51	99.11	99.75	99.11	100.92	100.08
CIA	33.67	35.06	41.06	37.11	71.06	73.21	70.94	72.25	57.95	75.45	71.40	60.26	75.75	75.14	76.64	61.87
PIA	27.50	34.89	34.25	24.85	97.80	98.59	98.74	97.80	76.45	96.96	98.41	64.66	96.99	97.72	97.01	65.71
CIW	39.02	35.26	52.40	49.06	98.66	99.09	99.24	98.60	89.11	97.86	99.05	70.89	97.87	98.42	97.84	70.49
ppm																
Sc	7.59	13.70	9.00	7.48	14.04	14.25	12.43	12.50	7.72	9.10	9.44	3.28	2.64	2.57	3.18	3.02
V	36.68	52.53	56.03	38.58	65.38	226.87	55.41	55.19	45.56	14.65	44.97	20.74	37.44	14.37	21.58	19.49
Cr	113.30	107.20	65.32	65.13	192.66	75.64	215.30	274.50	149.43	98.95	419.60	63.34	117.62	92.88	234.26	91.48
Co	8.06	11.09	10.71	8.58	15.43	9.65	12.92	12.98	4.62	3.80	8.21	3.01	0.95	1.64	2.40	3.89
Ni	56.37	32.42	37.30	32.74	32.87	27.80	32.95	72.69	29.24	7.27	55.84	20.35	15.47	16.83	18.81	7.38
Ba	660.70	89.98	887.60	1441.00	758.62	767.15	538.20	489.70	20201.16	679.51	627.80	955.40	355.25	177.46	212.55	711.60
Rb	118.70	8.32	131.50	107.00	248.15	215.42	256.90	195.90	328.26	139.21	165.40	137.30	88.18	93.11	48.98	85.58
Sr	89.54	109.80	95.77	194.50	44.28	31.92	54.30	65.23	198.02	94.60	47.18	171.39	21.08	24.49	37.60	149.80
Zr	197.10	79.49	188.70	253.50	219.49	334.46	183.80	193.00	150.97	398.71	278.20	128.99	75.75	44.94	99.15	110.50
Y	14.95	12.94	18.88	17.54	21.99	30.65	19.64	20.61	20.44	26.12	22.99	7.21	21.59	6.52	12.11	5.84
Th	10.68	4.93	9.96	10.64	19.33	16.33	18.38	17.57	13.57	14.83	13.98	9.70	14.42	3.59	5.14	6.26
U	2.44	1.38	2.09	2.50	2.77	3.37	1.76	2.34	2.08	0.49	2.11	1.04	2.49	0.55	0.88	1.42
Pb	5.52	8.18	2.88	11.23	10.74	33.63	10.02	5.12	54.18	128.08	7.90	25.87	4.47	6.50	13.30	7.41
Hf	5.47	2.41	5.09	6.60	6.09	9.02	5.24	5.49	4.18	9.93	7.11	3.82	2.22	1.31	2.68	3.11
Nb	7.33	8.27	7.17	7.12	12.08	13.26	9.81	10.36	9.37	12.88	10.04	5.39	6.79	5.14	3.38	4.30
Ta	0.81	0.83	0.72	0.73	1.51	1.45	1.10	1.15	0.91	1.34	1.08	0.45	1.17	0.89	0.44	0.55
La	25.68	9.88	36.36	27.46	46.61	27.82	46.89	37.10	24.80	35.03	49.75	19.99	26.77	9.83	15.21	20.56
Ce	49.08	20.42	56.19	52.37	90.08	60.98	69.35	70.23	53.67	66.16	68.68	37.30	54.32	21.64	30.58	34.58
Pr	5.63	2.89	7.33	6.10	9.97	6.92	9.68	7.90	6.50	7.69	10.33	4.22	6.28	2.40	3.51	3.66
Nd	20.14	11.86	26.24	22.33	35.79	25.56	34.27	27.79	25.63	27.88	37.16	14.83	22.86	8.85	13.26	12.51
Eu	0.71	0.56	0.93	0.82	1.23	1.07	1.12	0.99	1.34	1.28	1.26	0.69	0.76	0.29	0.54	0.62
Gd	2.84	2.40	3.63	3.33	4.92	4.73	4.51	4.18	3.73	4.74	5.00	1.88	3.66	1.29	2.27	1.60
Dy	2.60	2.28	3.27	3.03	4.20	5.39	3.90	3.74	3.36	5.01	4.10	1.37	3.67	1.05	2.16	1.17
Ho	0.54	0.47	0.68	0.63	0.83	1.19	0.76	0.78	0.72	1.08	0.83	0.27	0.80	0.21	0.48	0.21
Er	1.50	1.20	1.82	1.72	2.21	3.38	2.01	2.09	1.91	3.01	2.20	0.71	2.27	0.57	1.21	0.51
Yb	1.62	1.16	1.83	1.71	2.24	3.54	2.05	2.15	1.90	3.22	2.19	0.72	2.27	0.53	1.16	0.43
Lu	0.26	0.17	0.28	0.27	0.34	0.52	0.31	0.33	0.28	0.48	0.33	0.11	0.31	0.09	0.17	0.07
Sm	3.63	2.75	4.38	4.10	6.43	5.17	6.16	5.09	4.72	5.44	6.52	2.62	4.43	1.77	2.63	2.16
Tm	0.25	0.17	0.27	0.25	0.32	0.51	0.29	0.31	0.28	0.46	0.32	0.10	0.34	0.08	0.17	0.07
Tb	0.45	0.38	0.55	0.50	0.72	0.80	0.68	0.64	0.58	0.77	0.72	0.23	0.56	0.19	0.33	0.21
Cs	14.08	0.71	0.98	1.68	16.69	12.79	14.79	10.76	24.33	12.58	6.72	4.48	3.33	7.20	4.02	1.09
Eu/Eu*	0.67	0.66	0.70	0.68	0.66	0.66	0.65	0.65	0.97	0.77	0.67	0.94	0.59	0.58	0.68	1.01
(La/Yb)N	10.79	5.78	13.56	10.91	14.16	5.34	15.73	11.73	8.85	7.40	15.44	18.98	8.01	12.10	8.88	31.04
(Gd/Yb)N	1.42	1.67	1.61	1.58	1.78	1.08	1.80	1.57	1.59	1.19	1.85	2.12	1.51	1.90	1.58	2.88

6. Discussion

6.1. Weathering context and intensity

The Chemical Index Alteration (CIA), the Plagioclase Index Alteration (PIA) and the Chemical Index of weathering (CIW) proposed by Nesbit and Young (1982) and Fedo et al. (1995), can be used to determine the nature and degree of chemical weathering undergone by rocks in their area of origin. According to Fedo et al. (1995), fresh basalts are characterized by CIA values between 30 to 45%, granodiorites and granites have CIA values between 45 to 55%, CIA values between 60 to 80% indicate moderate alteration, while values above 80% indicate intense alteration in the source zone. In the metasedimentary rocks of the southern Ouaddaï studied, the CIA values ranging between 33.67 to 41.06% in the paragneisses, 57.94 to 75.45% in the metapelites and 60.26 to 76.64% in the phengite quartzites. These values show that the paragneisses are characterized by the absence of the weathering, while the metapelites and phengite quartzites are characterized by moderate weathering. The very high PIA values in the metapelites (76-99%) and phengite quartzites (64-98%) are identical to those in the CIW, which ranging between 89 to 99% and 70 to 98% respectively. This would explain the complete transformation of plagioclase into aluminous clay minerals such as kaolinite and illite (Fedo et al., 1995) and the high intensity of weathering in the source zone (Condie et al., 1993). The low PIA (24 - 35%) and CIW (35 - 52%) values in the paragneisses would explain the absence of weathering rock. In the $A1_2O_3$-CaO + Na_2O-K_2O ternary diagram (Figure 6a), the metasediments of southern Ouaddaï indicate weak to intermediate weathering in the source. Most of the metapelites and phengite quartzites lie along the A-K poles, between biotite and muscovite. The paragneisses show the absence of weathering and are derived from felsic rocks (granodiorite and granite). The intensity of weathering can also be determined by Th/U ratios. Values of Th/U ratios > 4 suggest a high intensity of weathering in the source zone of sedimentary rocks (McLennan et al., 1993). These values ranging between 3.6 to 4.8 in paragneisses and imply a low degree of weathering. Those for metapelites (4.8 - 30.5) and phengite quartzites (4.4 - 10.1) are relatively high and imply an intense degree of weathering produced by the rock. In the Th/U vs Th discrimination diagram (Figure 6b), the metasedimentary rocks of southern part of Ouaddaï are close to the contents of the upper crust and are aligned with the weathering trends of McLennan et al. (1993). These results explain that the metasedimentary rocks of the Ouaddaï are derived from the erosion of the surrounding cratons. This is consistent with the results obtained by Djerossem et al. 2021.

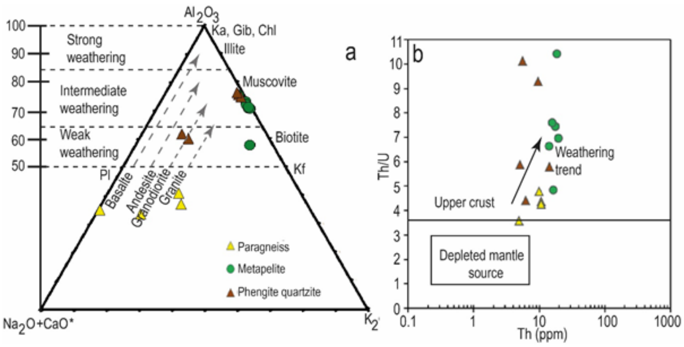

Figure 6 : a) Molecular proportions of Al_2O_3–(Na_2O + CaO*)–K_2O ternary diagram (Nesbitt et al., 1989) for the metasedimentary rocks of southern Ouaddaï formations with Chemical Index of Alteration (CIA) scale; b) Plot of Th/U ratios vs. Th after McLennan (1993).

6.2. Provenance

Al_2O_3/TiO_2 ratios can be used as an indicator to determine the provenance of sediments (Hayashi et al., 1997; Nagarajan et al., 2015). These ratios ($A1_2O_3$/TiO_2) range from 3 to 8 in mafic rocks, from 8 to 21 in intermediate rocks and from 21 to 70 in felsic rocks (Hayashi et al., 1997; Armstrong-Altrin et al., 2015a, b). $A1_2O_3/TiO_2$ ratios in the metasedimentary rocks of southern Ouaddaï range from 17 to 65% and suggest that the parent rocks were intermediate to felsic rocks, indicated in the TiO_2 vs Zr diagram (Figure 7a). The REE pattern normalized to chondrites, show an enrichment in LREE compared to HREE, a negative Eu anomaly, La/Sc ratios (0.72 - 9.42) > 0.7. These values show that the Southern Ouaddaï metasediments are consisted with a felsic source (Huntsman-Mapila et al., 2005). In addition, the felsic rocks are characterized by Ti/Zr < 20, Cr/Zr < 0.5, Cr/Th= 4 - 15, Th/Sc= 0.84 - 20.5, La/Sc= 2.5 - 16.3, Th/Co= 0.67 - 17.3 and La/Co= 1.8 - 13.8 (Culler et al., 2000). In the metasediments of southern Ouaddaï, Ti/Zr = 6.01 - 38.61 (average: 15.30), Cr/Zr = 0.22 - 2.36 (average: 1.01), Cr/Th = 4.62 - 45.53 (average: 14. 06), Th/Sc = 0.36 - 5.08 (average: 1.79), La/Sc = 0.72 - 9.42 (average: 4.20), Th/Co = 0.44 - 44.20 (average: 2.76) and La/Co = 0.89 - 28. 19 (average: 6.01). These results are identical to those for the felsic rocks and suggest that the metasediments studied come from an acid magmatic source as defined in the diagram of Floyd and Leveridge (1987) or all the samples fall within the acid arc source field and derive from an upper continental crust (Figure 7b).

6.3. Tectonic setting

Sediments are generally transported and deposited in different tectonic environments to those in which they originate (McLennan et al., 1993). A great deal of work based on geochemical characteristics (major, trace and rare earth elements) has been carried out to determine the tectonic environments in which sediments were deposited. In the K_2O/Na_2O vs SiO_2 discrimination diagram of Roser et al., 1986 (Fig.7c), the majority of metasediments (paragneisses, metapelites and phengite quartzites) fall in the field of the passive continental margin, with a minority of samples of phengite quartzites and paragneisses falling in the field of the active continental margin. One paragneiss sample fall into the field of the Island continental arc. This result explains why the metasediments of the southern Ouaddaï were formed in a passive to active continental margin tectonic environment. These results are identical to those obtained in Cameroon by Ngoniri et al., 2020. La/Th ratios can also be used to determine the tectonic environment of the sediments. Average La/Th ratios are 3.6 for Archean sedimentary rocks and 2.7 for post-Archean rocks (McLennan and Taylor, 1991). These ratios are highly variable in paragneisses (2 - 3.7; average: 2.7), metapelites (1.6 - 3.6; average: 2.3) and phengite quartzites (1.8 - 3.3; average: 2.4). This explains why the majority of the metasediments studied (paragneiss, metapelite, phengite quartzite) are close to a post-archean context, with only a few samples (paragneiss and phengite quartzite) corresponding to an Archean context. The La vs Th discrimination diagram of McLennan et al. (1989) also confirms the Archean to post-Archean context for the metasediments of southern Ouaddaï (Figure 7d). This is also compatible with the results obtained by Djerossem et al. (2021) to the southern Ouaddaï (Chad) and in Cameroon (Ngoniri et al., 2020; Fossi, (2023)) in metasedimentary rocks.

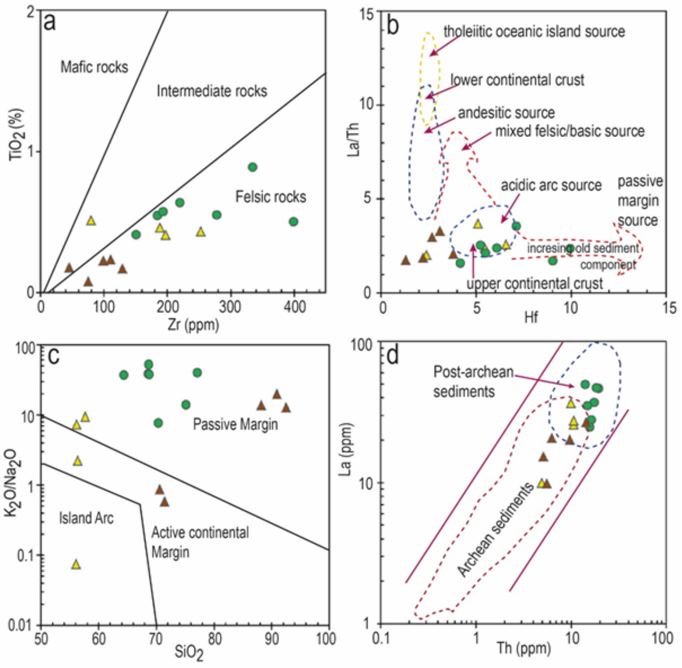

Figure 7: Source rocks discrimination diagram after Floyd et al. (1989): (a) TiO_2 versus Zr and (b) La/Th-Hf. (c) Tectonic discrimination diagrams of the southern Ouaddaï metasedimentary rocks: SiO_2/Al_2O_3 vs. K_2O / Na_2O. (d) La vs Th source rocks discrimination diagram for the metasedimentary rocks (Mc Lennan et al., 1989).

7. Conclusion

The southern Ouaddaï metasedimentary rocks are made up of paragneiss (garnet-biotite paragneiss, amphibole paragneiss and silicium silicate paragneiss), metapelite and phengite quartzite. The presence of mineral such as sillimanite is an excellent indicator of their sedimentary origin. Geochemical characteristics show that these metasediments correspond mainly to a protolith of greywackes and arkoses derived from a source rock of felsic composition. The CIA values indicate that these rocks have undergone a low to moderate degree of chemical weathering. On the other hand, the high PIA and CIW values indicate an intense degree of weathering. Based on Rare earths and trace elements results compared with those from Cameroon, we propose that the sedimentary rocks of the southern Ouaddaï are characterized by a protolith derived from an upper continental crust, deposited in an active to passive continental margin geodynamic environment.

Acknowledgements

This work is part of Félix Djerossem PhD thesis conducted at the Université Paul Sabatier, Toulouse 3 with a fellowship from the French Embassy in Chad. This work is part of the URCO project funded by the CNRS-NEEDS Program for field and analytical expenses. Fabienne de Parseval and Jean-François Ména are thanked for the confection of thin sections.

Reference

Armelle, N.F., Djibril K.N.G., Brice K.W. and Timoleon N. (2023). Petrochemical characterization of metasedimentary rocks in the Nkolkosse area, Yaoundé domain of the Pan-African fold belt in Cameroon: constrain on their provenance, protolith, and tectonic setting. Arabian Journal of Geosciences, 16, 654.

Armstrong-Altrin, J.S., Lee Y.L., Verma S.P. and Ramasamy S. (2004a) Geochemistry of sandstones from the upper Miocene Kudankulam formation, Southern India: implications for provenance, weathering and tectonic setting. Journal of Sediment Research, 74, 285–297.

Armstrong-Altrin, J.S., Lee Y.I., Verma S.P. and Ramasamy S. (2004b). Geochemistry of sandstones from the Upper Miocene Kudankulam Formation, Southern India: implications for provenance, weathering, and tectonic setting. Journal of Sediment Research, 74, 285–297.

Armstrong-Altrin, J.S., Machain-Castillo M.L., Rosales-Hoz L., Carranza Edwards, A., Sanchez-Cabeza J.A. and Ruiz-Fernandez A.C. (2015a). Provenance and depositional history of continental slope sediments in the Southwestern Gulf of Mexico unraveled by geochemical analysis. Cont Shelf Res 95:15–26.

Armstrong-Altrin, JS., Nagarajan R., Balaram V. and Natalhy-Pineda O. (2015b). Petrography and geochemistry of sands from the Chachalacas and Veracruz beach areas, Western Gulf of Mexico, Mexico: constraints on provenance and tectonic setting. J S Am Earth Sci 64:199–216.

Bhatia M.R. and Crook K.A. (1986). Trace element characteristics of greywackes and tectonic setting discrimination of sedimentary basins. Contribution to Mineralogy and Petrology, 92, 181-193.

Carignan, J., Hild P., Mevelle G., Morel J. and Yeghicheyan D. (2001). Routine analyses of trace elements in geological samples using flow injection and low pressure on-line liquid chromatography coupled to ICP-MS: A study of geochemical reference materials BR, DR-N, UB-N, AN-G and GH. Geostand. Newslett., 25, 187–198.

Condie K.C. (1993). Chemical composition and evolution of the upper continental crust: contrasting results from surface samples and shales. Chem Geol, 104, 1–37.

Cullers R.L. (2000). The geochemistry of shales, siltstones and sandstones of Pennsylvanian-Permian age, Colorado, USA: implications for provenance and metamorphic studies. Lithos, 51, 181–203

Djerossem, F., Zeh A., Isseini M., Vanderhaeghe O., Berger J. and Ganne J. (2021). U-Pb-Hf isotopic systematics of zircons from granites and metasediments of southern Ouaddaï (Chad), implications for crustal evolution and provenance in the Central Africa Orogenic Belt. Precambrian Research, 361, 106233.

Djerossem, F., Berger J., Vanderhaeghe O., Isseini M., Ganne J. and Zeh A. (2020). Neoproterozoic magmatic evolution of the southern Ouaddaï Massif (Chad). Bulletin de la Société Geologique de France (BSGF) 191, 34.

Djerossem N.F. (2018). Croissance et remobilisation crustales au Pan-Africain dans le Sud du massif du Ouaddaï au Tchad. Thèse de doctorat Phd à l'Université Paul Sabatier de Toulouse (France), 302pp.

Dunlap W.J., Teyssier C., Hirth J.G. and McDougall I. (1995). Thermal, mechanical and kinematic evolution of a ductile duplex: Ruby Gap Duplex, central Australia, Geol. Soc. Aust.Abstr, 40, 39-40.

Fedo C.M., Nesbitt H.W. and Young G.M. (1995). Unraveling the effects of potassium metasomatism in sedimentary rocks and paleosols, with implications for paleoweathering conditions and provenance. Geology, 23(10), 921.

Floyd P.A. and Leveridge B.E. (1987). Tectonic environment of the Devonian Gramscatho Basin, South Cornwall: framework mode and geochemical evidence from turbiditic sandstones. J Geol Soc Lond, 144, 531–542.

Fossi D.H. (2023). Pétrogenèse et structuogénèse des formations de Deng-Deng (Est-Cameroun). Thèse de doctorat Phd à l'Université de Yaoundé I (Cameroun), 180pp.

Gsell J. and Sonnet J. (1960). Carte géologique de reconnaissance au 1 I 500.000 et Notice explicative sur la feuille Adre. Brazzaville, BRGM, 42 pages.

Hayashi, KI., Fujisawa H., Holland H.D. and Ohmoto H. (1997). Geochemistry of ~1.9 Ga sedimentary rocks from northeastern Labrador, Canada. Geochim Cosmochim Acta, 61, 4115–4137.

Herron M.M. (1988). Geochemical classification of terrigenous sands and shales from core or log data. J Sediment Petrol 58:820–829.

Hirth G. and Tullis J. (1992). Dislocation creep regimes in quartz aggregates. Journal of Structural Geology, 14, 2, 145-159.

Huntsman-Mapila, P., Kampunzu A.B., Vin k.B. and Ringrose S. (2005). Cryptic indicators of provenance from the geochemistry of the Okavango Delta sediments, Botswana. Sed Geol, 174, 123–148.

Kogbe C.A. (1981). Cretaceous and Tertiary of the Iullemmeden Basin in Nigeria (West Africa): Cretaceous Research, v. 2, p. 129–186, doi: 10 .1016 /0195 -6671 (81)90007 -0.

McLennan, S.M., Hemming, S., Taylor, S.R. and Eriksson, K. A. (1995). Early Proterozoic crustal evolution: geochemical and Nd-Pb isotopic evidence from metasedimentary rocks, southwest ern North America. Geochimica et Cosmochimica Acta, 59, 1153-1177.

McLennan, S.M., Hemming S., McDaniel D.K. and Hanson G.N. (1993). Geochemical approaches to sedimentation, provenance and tectonics. In: Johnsson MJ, Basu A (eds) Processes controlling the composition of clastic sediments: Geological Society of America special paper, 284, 21–40.

McLennan S.M. and Taylor S.R. (1991). Sedimentary rocks and crustal evolution: tectonic setting and secular trends. J Geol, 99(1), 1–21.

McLennan S.M. (1989). Rare earth elements in sedimentary rocks: influence of provenance and sedimentary processes. In: Lipin, B.R, MacKay, G.A (eds) Geochemistry and mineralogy of rare earth elements. Mineral Soc Am, Chantilly, pp 169–200.

Milesi, J.P., Frizon de Lamotte D., De Kock G. and Toteu F. (2010). Tectonic Map of Africa: Paris, Commission de la carte géologique du monde/Commission for the Geological Map of the World (CCGM/CCGM), scale 1:10,000,000.

Miryam, T., Koffi A.M.P., Augustin K.Y., Nestor H., Ephrem A.M. and Roland K.B. (2023). Tracing the Origin of Metasedimentary Rocks in the Tortiya Diamond Region (Northern Côte d'Ivoire). Open Journal of Geology, 13, 1271-1290. https://doi.org/10.4236/ojg.2023.1312055

Nagarajan, R., Armstrong-Altrin J.S., Kessler F.L., Hidalgo-Moral E.L., DodgeWan D. and Taib N.I. (2015). Provenance and tectonic setting of Miocene siliciclastic sediments, Sibuti formation, northwestern Borneo. Arab J Geosci, 8(10), 8549–8565

Nesbitt H.W. and Young G.M. (1982). Early Proterozoic climates and plate motions inferred from major element chemistry of lutites. Nature, 299(5885), 715–717.

Ngoniri, A.H., Ngnotue T., Njiosseu E.L.T., Kenne P.A., Ganno S. and Nzenti J.P. (2020). Geochemistry of the Neoproterozoic Mbondo-Ngazi Tina Metasediments, Adamawa Area, Central Cameroon: Source Provenance and Tectonic Setting. Journal of Geosciences and Geomatics, 2, 94-109.

Roser B.P. and Korsch R.J. (1986). Determination of tectonic setting of sandstone-mudstone suites using SiO2 content and K2O/Na2O ratio. Journal of Geology, 94, 635-650.

Verma S.P., Pandarinath K. and Rivera-Gomez M.A. (2016). Evaluation of ongoing rifting and subduction processes in the geochemistry of magmas from the western part of the Mexican Volcanic Belt. J S Am Earth Sci, 66, 125–148.

Winchester J.A., Park K.G. and Holland J.G. (1980). The geochemistry of Levisian semipelitic schists from the Gairloch district western Ross. Scot J Geol, 16, 165–179.

Zeng, S., Wang J., Chen W., Fu X., Feng X., Song C., Wang D. and Sun W. (2019). Geochemical characteristics of early Cretaceous marine oil shale from Changshe Mountain area in the northern Qiangtang Basin, Tibet: implication for palaeoweathering, provenance, tectonic setting, and organic matter accumulation. Geol J, 55(1), 1–18.